

from sulfur (0.162  $e^-$ ), carbons (0.408  $e^-$ ), and even from hydrogens (0.104  $e^-$ ). By comparing the populations of the complex with the respective ones in thiophene and  $\text{Mo}(\text{CO})_3$  (see values in parentheses in Table III), we can obtain information on the effects of the interaction thiophene- $\text{Mo}(\text{CO})_3$  (horizontal chemisorption of thiophene on a one-center site). The CO ligands transfer less charge to the metal. The transfer to the Mo atom is mainly to the sp orbitals. The electronic sulfur drift is from the sp orbitals having also an increase of the d population. These results insinuate that the transfer from thiophene is mainly through the sp-sp interactions, as shown in Figure 7, although, another more complex mechanism cannot be discarded.

The transfer of charge from thiophene to the metal may be interpreted as an indication of the weakening of thiophenic bonds. In fact, recent experimental studies of thiophene adsorption on crystal surfaces of  $\text{Mo}^{6,8,47}$  and on a  $\text{MoO}_3/\gamma\text{-Al}_2\text{O}_3$  catalyst<sup>48</sup> reveal that the chemisorption at low coverage (parallel adsorption) is irreversible, and a decomposition of thiophene is observed. In general, at low coverage, the heat of adsorption is the highest owing to the fact that the adsorption sites are the most unsaturated ( $\text{Mo}(\text{CO})_3$ ). As the coverage increases close to saturation, only those sites that have a vacancy with one unsaturation are available ( $\text{Mo}(\text{CO})_5$ ), and the heat of adsorption is smaller due to a weaker bond adsorbate-substrate and a repulsive interaction adsorbate-adsorbate. A very important fact in relation to the reactivity of chemisorbed thiophene during HDS concerns the nature of the  $16a'$  (LUMO) orbital of  $\text{Mo}(\eta^5\text{-thiophene})(\text{CO})_3$  which is 73% located on the thiophenic ring, mainly on C-S bonds, and has an antibonding character. This suggests that nucleophilic attack to  $C_1$  or  $C_4$  can result in C-S bond scission, as occurs in nucleophilic reactions of the complex  $[(\eta^5\text{-C}_5\text{H}_5)\text{Ru}(\eta^5\text{-thiophene})]^+ 14^d$  and of thiophenic molecules in general.<sup>49</sup> This supports the view that hydrogenolysis of C-S bonds is probably the step following chemisorption during HDS of thiophene. In the case of Mo-

$(\text{CO})_5(\eta^1\text{-thiophene})$ , the HOMO ( $9b_1$ ) is 70% on the Mo-S bond and the LUMO ( $12b_2$ ) is an orbital located on CO bonds, hence the activation of thiophenic bonds toward nucleophilic attack is not expected.

The analysis of the bond orders in Table III indicates that the bond between thiophene and Mo in  $\text{Mo}(\eta^5\text{-thiophene})(\text{CO})_3$  is chiefly sp-sp with some contributions of sp-d (Mo-C<sub>1</sub>, Mo-C<sub>2</sub>, and Mo-S bonds) and d-d (Mo-S bond). Again, the sulfur d-orbitals take part in the bonds through sp-d and d-d bonding interactions, see Figure 7.

It is also observed that the Mo-CO bond orders do not change by interaction of  $\text{Mo}(\text{CO})_3$  with thiophene. The C<sub>1</sub>-S, C<sub>1</sub>-C<sub>2</sub>, and C<sub>2</sub>-C<sub>3</sub> bonds have greater changes than in the  $\eta^1$ -complex, but as we noted in the previous section, geometrical relaxation would be necessary to observe a noticeable variation in the bond orders.

### Conclusions

(a) Our results suggest that although the complexes  $\text{Mo}(\eta^1\text{-S-thiophene})(\text{CO})_5$  and  $\text{Mo}(\eta^5\text{-thiophene})(\text{CO})_3$  have not been synthesized as yet, their formation is possible.

(b) The nature of the thiophene-metal bond is mainly sp-sp with some d-d and sp-d contributions. The d-sulfur orbitals participate in the metal-thiophene bond.

(c) There is a small transfer of charge from the metal to thiophene in the  $\eta^1\text{S}$ -complex and a noticeable drift of charge from thiophene to molybdenum in the case of the  $\eta^5$ -complex.

(d) The binding energy of thiophene in the  $\text{Mo}(\eta^5\text{-thiophene})(\text{CO})_3$  is greater than in  $\text{Mo}(\eta^1\text{S-thiophene})(\text{CO})_5$ , which correlates well with surface chemistry results.

(e) Activation of the C-S bonds of thiophene toward nucleophilic attack at  $C_1$  or  $C_4$  is expected in the case of  $\text{Mo}(\eta^5\text{-thiophene})(\text{CO})_3$ , whereas no such activation is apparent for  $\text{Mo}(\eta^1\text{S-thiophene})(\text{CO})_5$ .

**Acknowledgment.** This research could not have been accomplished without CONICIT's grants, S1-1846 and S1-1814, and the computational facilities of IVIC and IBM Scientific Center.

**Registry No.**  $\text{Mo}(\text{CO})_5(\eta^1\text{-thiophene})$ , 117095-45-1;  $\text{Mo}(\text{CO})_3(\eta^5\text{-thiophene})$ , 117095-46-2.

(47) Gellman, A. J.; Farias, M. J.; Salmeron, M.; Somorjai, G. A. *Surf. Sci.* **1984**, *136*, 217.

(48) Vattis, D.; Matralis, H.; Lycorghiotis, A. *J. Chem. Soc., Faraday Trans. 1* **1987**, *83*, 1179.

(49) Meth-Cohn, O. In *Comprehensive Organic Chemistry*; Sammes, P. G., Ed.; Pergamon Press: Oxford, **1979**; p 804.

## Surface Dynamics of Adsorbed Species on Heterogeneous Oxidation Catalysts: Evidence from the Oxidation of $C_4$ and $C_5$ Alkanes on Vanadyl Pyrophosphate

Guido Busca<sup>†</sup> and Gabriele Centi\*

Contribution from the Department of Industrial Chemistry and Materials, University of Bologna, Viale Risorgimento 4, Bologna, Italy. Received December 18, 1987

**Abstract:** Steady-state and transient reactivity measurements, Fourier-transform infrared studies, and stopped-flow desorption analyses of the selective oxidation of  $C_4$  and  $C_5$  alkanes at the vanadyl pyrophosphate surface suggest that the surface dynamics of adsorbed species plays an important role in determining the selective oxidation pathways and the nature of the products of selective oxidation. The results indicate the possibility of two different oxidation pathways in maleic anhydride synthesis from *n*-butane which involve the intermediate formation of either a lactone or furan and which are characterized by different rates and selectivities. The presence of side methyl groups in the formation of similar intermediates from *n*-pentane decreases their reactivity and favors a parallel surface reaction between intermediates with the final formation of phthalic anhydride from the  $C_5$  hydrocarbon. However, when the rate of conversion of the intermediates is increased, thus modifying the surface availability of oxygen, maleic anhydride also becomes the principal product from the  $C_5$  alkane.

Recent developments of in situ characterization of adsorbed species during catalytic heterogeneous processes highlight their role in the self-organization of active surfaces (coadsorption enhancement effects, cocatalysis by strongly adsorbed substances,

...) as well as the influence of their surface mobility. For example, recent studies have shown<sup>1d</sup> the high rate of surface diffusion on

<sup>†</sup> Institute of Chemistry, College of Engineering, University of Genoa, Fiera del Mare, Genoa, Italy.

(1) (a) Zaera, F.; Gellman, A. J.; Somorjai, G. A. *Acc. Chem. Res.* **1986**, *19*, 24. (b) Pimental, G. *Chem. Technol.* **1986**, *9*, 536. (c) Davis, S. M.; Zaera, F.; Somorjai, G. A., *J. Catal.* **1982**, *77*, 439. (d) Cevallos-Candau, J. F.; Conner, W. C. *J. Catal.* **1987**, *106*, 376.

SiO<sub>2</sub> of H atoms produced by H<sub>2</sub> spillover on a point source. A catalytically active surface, therefore, is a bidimensional "adsorbed species-solid surface structure" in dynamic equilibrium. However, the role of surface concentration and mobility of adsorbed species often is not considered, especially for reactions of heterogeneous selective oxidation.<sup>2</sup> Heterogeneous oxidation reactions are complex multistep reactions. The selective transformation of *n*-butane to maleic anhydride<sup>3-5</sup> is a 14-electron oxidation with abstraction of 8 hydrogen atoms and insertion of 3 oxygen atoms. The transformation apparently occurs in one step without the appearance of detectable intermediates in the gas phase. Owing to the low reactivities of alkanes, the rate-determining step is the removal of the first paraffinic hydrogen from the *n*-butane.<sup>4,6-8</sup> The consecutive steps up to the formation of maleic anhydride are assumed to be much faster. The selectivity in maleic anhydride formation is determined by the rate of its consecutive oxidation to carbon oxides or of direct butane oxidation to CO<sub>x</sub>. The selectivity is thus independent of the rate of transformation of the adsorbed intermediates up to the formation of maleic anhydride. In addition, the surface concentration of these adsorbed intermediates is assumed not to be significant. Recently, however, we have presented some evidence<sup>2</sup> indicating that selectivity can be influenced by the surface concentration of these reaction intermediates. A further suggestion of the role of surface reactions is derived from a recent short communication.<sup>9</sup> On the same, very active and selective catalyst for *n*-butane (C<sub>4</sub>H<sub>10</sub>) oxidation to maleic anhydride (C<sub>4</sub>H<sub>2</sub>O<sub>3</sub>), the oxidation of *n*-pentane (C<sub>5</sub>H<sub>12</sub>) selectively gives the C<sub>8</sub> product phthalic anhydride (C<sub>8</sub>H<sub>4</sub>O<sub>3</sub>) and the C<sub>4</sub> product maleic anhydride. The increase of the carbon atom number necessarily involves C-C bond formation reactions between reactant or product molecules and/or adsorbed intermediates. However, this reaction (phthalic anhydride formation) is specific for *n*-pentane.<sup>9</sup> Butane or butadiene, for example, gives only very low yields of phthalic anhydride and very high selectivities to maleic anhydride. This indicates that the Diels-Alder reaction between butadiene and maleic anhydride does not occur. Probably the predominant mechanisms of phthalic anhydride formation are templating surface reactions between adsorbed intermediates.

In conclusion, some literature data indicate that the dynamics of surface reactions of adsorbed species play a central role in determining selectivity during heterogeneous alkane oxidation. The aim of this work was to study these concepts further by combining spectroscopic and surface reactivity measurements in the selective oxidation of C<sub>4</sub> and C<sub>5</sub> alkanes. The catalyst used for the study is an optimized vanadyl pyrophosphate catalyst highly active and selective in the transformation of *n*-butane to maleic anhydride.<sup>10,11</sup> Principal goals of this research were to (i) study the fundamental aspect of the nature and presence of relevant amounts of adsorbed intermediates even in the presence of gaseous oxygen, (ii) show that the active sites on the oxide surface may

be comprised by both the catalyst itself and the adsorbed intermediates, and (iii) obtain a better understanding of the mechanistic aspects of the selective oxidation of *n*-butane to maleic anhydride.

### Experimental Section

**(VO)<sub>2</sub>P<sub>2</sub>O<sub>7</sub> Preparation.**<sup>10</sup> Vanadium pentoxide (50 g from Merck) was stirred into 0.6 L of a technical-grade mixture (1:2) of benzyl and isobutyl alcohols. Orthophosphoric acid (in such an amount as to give a final atomic P:V ratio of 1.1) dissolved in 0.1 L in isobutyl alcohol was then added to form a slurry which gradually darkened upon heating to the reflux temperature (approximately 378 K). After several hours, the mixture was cooled with continued stirring. The light-green product was isolated by filtration, washed, and then dried overnight at 333 K. Both X-ray diffraction patterns and infrared examination indicated the solid to be [VOHPO<sub>4</sub>]<sub>2</sub>H<sub>2</sub>O.<sup>10,12-14</sup> The vanadyl hydrogen phosphate hemihydrate was then calcined at 673 K in a mixture of 1.5% butane/air until steady-state conversion of butane to maleic anhydride was well established. The reactor was then cooled; the solid recovered was shown to be pure (VO)<sub>2</sub>P<sub>2</sub>O<sub>7</sub><sup>10</sup> by chemical, infrared, and X-ray diffraction analyses. Further details on the characterization of the catalyst and its redox properties as well as catalytic behavior in the oxidation of *n*-butane to maleic anhydride have been previously reported.<sup>8,10,11,15</sup>

**Reactivity Measurements.** Reactivity measurements in steady-state conditions and in unsteady-state conditions were made with a continuous flow fixed-bed integral reactor and with a pulse-type reactor, respectively.

The flow reactor was charged with 6 g of sample with particle dimensions in the 0.125–0.250-mm range. The reactor was provided with an axial thermocouple sliding inside in order to control its isothermicity during catalytic runs. The absence of significant diffusional limitations (heat and mass transfer) on the rate of hydrocarbon depletion was experimentally verified. Catalytic data refer to steady-state behavior constant for at least 100 h.

The pulse reactor was charged with 0.5 g of sample with an height-to-width ratio chosen in order to minimize the effects of concentration and temperature differences along the catalytic bed (differential mode). The reactor temperature was determined at the midpoint of the catalytic bed.

The reactor assembly was interfaced between the section of reagent mixture preparation and flow control and the section of the on-line gas chromatographic analyses of the reaction products. The outlet stream from the reactor was kept at 493 K to prevent condensation of organic products that were analyzed in a first gas chromatograph (GC) using a flame ionization detector. After cooling of the gas stream, oxygen, nitrogen, CO, and CO<sub>2</sub> were analyzed in a second gas chromatograph using a thermoconductibility detector. A 3-m long Porapak QS column was utilized in the first GC. Oven temperature was programmed to rise from 353 to 503 K at a rate of 16 K min<sup>-1</sup>. The second GC operated with a Carbosieve-II column. Oven temperature was programmed from room temperature to 503 K at a rate of 32 K min<sup>-1</sup> after an initial 9 min under isothermal conditions.

**Fourier-Transform Infrared Spectra (FT-IR).** Infrared spectra (self-supporting disk technique) were recorded with a Nicolet MX1 Fourier-transform spectrometer (resolution 1 cm<sup>-1</sup>), equipped with a conventional gas manipulation and evacuation line and IR cells, allowing measurements up to 870 K. The usual pretreatment of the samples was evacuation at 723 K at 10<sup>-5</sup> Torr. Adsorbate compounds were hyperpure products from Carlo Erba and SIO (Milano, Italy). Self-supporting disks (about 10–20 mg cm<sup>-2</sup>) for infrared examination were prepared by pressing the calcined samples at 20 000 psi.

**Desorption Studies.** Desorption studies were made utilizing the technique of "stopped-flow desorption"<sup>16</sup> (SFD). This technique consists of the gas chromatographic analysis of the products of thermal desorption in an unreactive flow (deoxygenated helium flow) from a catalyst surface subjected to a rapid switching from flow steady-state catalytic conditions to those for the desorption. The catalyst (0.5 g) was charged in a flow isothermal microreactor, and, after attainment of steady-state catalytic behavior through a series of valves, the reactor was put directly on-line to a gas chromatograph column whose head was maintained at a low

(2) For a general discussion of the problem, see: Cavani, F.; Centi, G.; Trifirò, F.; Grasselli, R. Preprints of the Symposium on Hydrocarbon Oxidation, 194th National Meeting of the American Chemical Society, New Orleans, 1987 (Division of Petroleum Chemistry); p 811, *Catal. Today*, in press.

(3) (a) Hodnett, B. K. *Catal. Rev. Sci.-Eng.* **1985**, *27*, 373. (b) Ai, M. *J. Catal.* **1986**, *100*, 336. (c) Moser, T. P.; Schrader, G. L. *J. Catal.* **1985**, *92*, 216. (d) Shimoda, T.; Okuhara, T.; Misono, M. *Bull. Chem. Soc. Jpn.* **1985**, *58*, 2163. (e) Hodnett, B. K.; Delmon, B. *Ind. Eng. Chem. Fundam.* **1984**, *23*, 465.

(4) Pepera, M. A.; Callahan, J. L.; Desmond, M. J.; Milberger, E. C.; Blum, P. R.; Bremer, N. J. *J. Am. Chem. Soc.* **1985**, *107*, 4883.

(5) (a) Centi, G.; Trifirò, F.; Ebner, J. R.; Franchetti, V. *Chem. Rev.* **1988**, *88*, 55. (b) Centi, G.; Trifirò, F. *Chim. Ind. (Milan)* **1986**, *68*, 74.

(6) (a) Wenig, R. W.; Schrader, G. L. *Ind. Eng. Chem. Fundam.* **1986**, *25*, 612.

(7) (a) Buchanan, J. S.; Sundaresan, S. *Appl. Catal.* **1986**, *26*, 211. (b) Nechiporuk, P. P.; Mishchenko, Yu. A.; Avetisov, A. K.; Dulin, D. A.; Kalinowski, I. O.; Gel'bshtein, A. I. *Kinet. Catal.* **1987**, *27*, 1304.

(8) Centi, G.; Fornasari, G.; Trifirò, F. *Ind. Eng. Chem. Prod. Res. Dev.* **1985**, *24*, 32.

(9) Burattini, M.; Centi, G.; Trifirò, F. *Appl. Catal.* **1987**, *32*, 353.

(10) Busca, G.; Cavani, F.; Centi, G.; Trifirò, F. *J. Catal.* **1986**, *99*, 400.

(11) Cavani, F.; Centi, G.; Riva, A.; Trifirò, F. *Catal. Today* **1987**, *1*, 17.

(12) Johnson, J. W.; Johnston, D. C.; Jacobson, A. J.; Brody, J. F. *J. Am. Chem. Soc.* **1984**, *106*, 8123.

(13) Torardi, C. C.; Calabrese, J. C. *Inorg. Chem.* **1984**, *23*, 1308.

(14) (a) Bordes, E.; Courtine, P.; Johnson, J. W. *J. Solid State Chem.* **1984**, *55*, 270. (b) Bordes, E.; Courtine, P. *J. Chem. Soc., Chem. Commun.* **1985**, 294. (c) Leonowicz, M. E.; Johnson, J. W.; Brody, J. F.; Shannon, H. F.; Newsam, J. M. *J. Solid State Chem.* **1985**, *56*, 370.

(15) Cavani, F.; Centi, G.; Trifirò, F. *J. Chem. Soc., Chem. Commun.* **1985**, 492.

(16) Busca, G.; Centi, G.; Trifirò, F. In *Catalyst Deactivation in 1987*; Delmon, B., Froment, G. F., Eds.; Elsevier: Amsterdam, 1987; p 427.

**Table I.** Comparison of the Steady-State Catalytic Behavior of Vanadyl Pyrophosphate in a Flow Reactor in the Oxidation of *n*-Butane and *n*-Pentane<sup>a</sup>

hydrocarbon	conversion	reaction temp, K	selectivity <sup>b</sup>			
			MA	PA	BA	CO <sub>x</sub>
<i>n</i> -butane	0.40	560	0.72			0.27
<i>n</i> -butane	0.80	580	0.63			0.38
<i>n</i> -pentane	0.40	565	0.22	0.36	0.02	0.38
<i>n</i> -pentane	0.80	590	0.20	0.28	0.12	0.41

<sup>a</sup> Experimental conditions: 2.3% v/v of hydrocarbon, 23% v/v of oxygen, 74.7% v/v of helium; 6 g of catalyst; total flow rate at STP conditions,  $12.3 \times 10^{-3}$  L min<sup>-1</sup>. <sup>b</sup> Selectivity to maleic anhydride,  $S =$  moles of maleic anhydride formed/moles of *n*-pentane consumed. Selectivity to phthalic anhydride or benzoic acid,  $S = 2 \times$  moles of product formed/moles of *n*-pentane consumed (the synthesis of these two products involves two molecules of hydrocarbon for the formation of one molecule of product). Selectivity to carbon oxides was calculated on the carbon basis. Note: MA, maleic anhydride; PA, phthalic anhydride; BA, benzoic acid; CO<sub>x</sub>, carbon oxides.

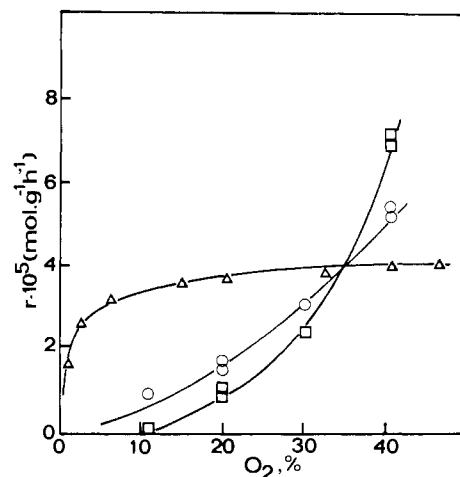
temperature to trap the desorbed products.

The experimental sequence for the SFD experiments was as follows. (a) With the apparatus and reactor working in continuous flow conditions, the catalyst was conditioned for around 6 h in a continuous flow of 2% *n*-butane in air at 573 K (up to achievement of steady-state catalytic conditions). (b) For a period of 2–5 min an equal flow of oxygen- and water-free helium was sent to the reactor in order to remove the gas phase and organic species weakly interacting with the surface. (c) The reactor was placed directly on-line to a gas chromatographic column (continuous flow of oxygen- and water-free helium) by contemporaneous switching of a series of valves. (d) The isothermal desorption products (at the same temperature as the catalytic tests, 573 K) were collected in a cold trap and after 2–3 h analyzed with a FID gas chromatograph. (e) After stage d, the temperature of the reactor was increased linearly up to a final temperature of 723 K, still under oxygen-free helium flow; the desorption products were collected in the cold trap and finally analyzed. These two fractions were called first and second fractions in the following discussion of the results.

## Results

**Reactivity Measurements. (a) Steady-State Oxidation.** The behavior of the vanadyl pyrophosphate in the steady-state oxidation of *n*-butane and *n*-pentane is compared in Table I. In *n*-butane conversion, in addition to maleic anhydride and carbon oxides, only traces of acetic acid and acetaldehyde were detected. *n*-Pentane under the same conditions led to the formation of maleic anhydride and phthalic anhydride and lower yields of benzoic acid. The activities of the catalyst in the conversion of the two alkanes are quite comparable as well as global selectivity (maleic anhydride + benzoic acid in *n*-butane oxidation and maleic anhydride + phthalic anhydride + benzoic acid in *n*-pentane oxidation). In both cases, selectivity decreased at conversions higher than about 80% with a parallel increase in the formation of carbon oxides, an effect usually observed in *n*-butane oxidation.<sup>7,8</sup> The catalyst is very active and the two alkanes were converted to selective products in a very low range of temperatures. These data indicate that the catalytic behavior of the catalyst is stable and compares well (in *n*-butane oxidation) with those of the patented catalysts.<sup>3</sup> On this catalyst and under the same reaction conditions, the oxidation of *n*-pentane led to the synthesis of an oxidized product with fewer carbon atoms than the starting alkane (C<sub>4</sub>, maleic anhydride) and products with a greater number of atoms (C<sub>8</sub>, phthalic anhydride; C<sub>7</sub>, benzoic acid). No reaction products with the same number of carbon atoms as the starting alkane (C<sub>5</sub>) were detected in the oxidation of *n*-pentane.

The effect of oxygen concentration on the rate of formation at 563 K of maleic anhydride from *n*-butane and maleic anhydride and phthalic anhydrides from *n*-pentane is reported in Figure 1. It is shown that the *n*-butane oxidation follows the usual Langmuir–Hinshelwood dependence on oxygen concentration, whereas an exponential dependence with a reaction order higher than one is shown by the *n*-pentane oxidation. This unusual kinetic behavior of the *n*-pentane necessarily implies more complex surface reaction phenomena involving oxygen, like that found, for example, in coadsorption enhancements or in competitive inhibition effects.<sup>17</sup>

**Figure 1.** Effect of oxygen partial pressure on the rates of formation at 563 K of maleic anhydride from *n*-butane ( $\Delta$ ) and of maleic anhydride ( $\square$ ) and phthalic anhydride ( $\circ$ ) from *n*-pentane.**Table II.** Comparison of the Kinetic Constants for a First-Order Rate of Hydrocarbon Depletion, Determined in Steady-State Flow Tests and in Unsteady-State Pulse Reactor Experiments<sup>a</sup>

hydrocarbon	first-order rate constant, L s <sup>-1</sup> g <sup>-1</sup>		
	steady-state flow oxidation	unsteady-state pulse reactor <sup>b</sup>	
		A	B
<i>n</i> -butane	$4.779 \times 10^{-5}$	$4.890 \times 10^{-5}$	$26.743 \times 10^{-5}$
<i>n</i> -pentane	$4.335 \times 10^{-5}$	$0.890 \times 10^{-5}$	$26.330 \times 10^{-5}$

<sup>a</sup> Experimental conditions: temperature of reaction, 573 K; 0.87 g of catalyst; total flow rate,  $30 \times 10^{-3}$  L min<sup>-1</sup>; steady-state oxidation, as in Table I; unsteady-state oxidation, each pulse (1 cc) containing 2.18% v/v *n*-butane in helium; carrier gas, deoxygenated helium. Data refer to activity for the first pulse. For the pulse reactor tests, in both cases a catalyst was used after the continuous-flow reactor oxidation of butane. However, in case A the pretreatment of the catalyst was at 573 K in helium flow (2 h), whereas in case B the catalyst was first brought up to 723 K in helium flow (1 h) and then cooled (always in helium flow) at 573 K for the pulse experiments. <sup>b</sup> Type of pretreatment of the catalyst in helium flow: (A) 2 h at 573 K; (B) 30 min at 723 K and then cooled at 573 K in helium for the pulse reactor experiments. The catalyst for pulse reactor experiments had first worked in steady-state conditions for at least 10 h.

**(b) Unsteady-State Oxidation.** Reported in Table II are the kinetic constants for the rate of *n*-butane depletion determined in the case of steady-state oxidation (aerobic conditions) in a flow reactor and in the case of unsteady-state oxidation (anaerobic conditions) in a pulse reactor after two different catalyst pretreatments. In both cases the starting catalyst had worked for at least 6 h in a continuous-flow reactor in butane oxidation.

Two main observations can be made from the data reported in Table II. (a) For *n*-butane, the data from the flow reactor and pulse reactor experiments are comparable. The former are obtained in a flow of hydrocarbon/oxygen and the latter in the absence of gaseous oxygen. The kinetic constants determined in the flow tests and in the pulse tests (A) are similar. Case A refers to a catalyst after continuous-flow oxidation and successive treatment in a flow of helium at the same temperature as that of the catalytic tests. In the first pulse, the rate of *n*-butane oxidation (case A) is not substantially affected by the absence of gaseous oxygen. This means that in these conditions the rate of hydrocarbon oxidation by lattice oxygen is not affected by the rate of catalyst surface reoxidation by gaseous oxygen.

(b) The activity in *n*-butane oxidation is enhanced considerably when the catalyst is first treated at higher temperatures in helium flow. This last effect also occurs in the oxidation of *n*-pentane (Table II), but in this case the activity in the pulse reactor (case A) is much lower than in steady-state conditions. This suggests

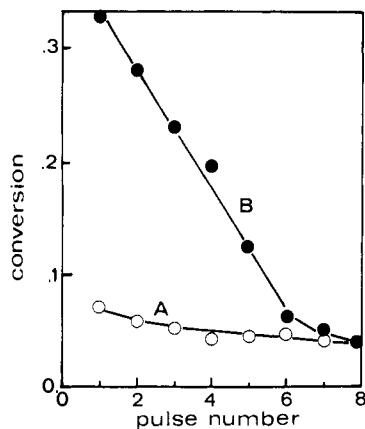


**Figure 2.** Conversion of *n*-butane in a pulse reactor in anaerobic conditions as a function of the number of pulses (each pulse  $0.912 \times 10^{-6}$  mol of butane in helium): (A) catalyst discharged by the continuous flow catalytic reaction (butane/air mixture at 573 K); (B) same catalyst as in case A, but before the tests in the pulse reactor the adsorbed species were removed by high-temperature treatment in an unreactive flow (see text).

that in *n*-pentane conversion the presence of oxygen has a considerable effect on the rate of hydrocarbon oxidation. The effect of oxygen in *n*-butane oxidation is much less. This is in agreement with the different kinetic behaviors with respect to oxygen partial pressure reported in Figure 1.

The different catalytic behaviors in the pulse reactor of the catalyst after different pretreatments (cases A and B) is confirmed in Figure 2, where the conversion of *n*-butane versus the number of pulses is reported. In both cases a decrease in activity is observed. For the catalyst pretreated at higher temperature (case B), a higher initial activity is found which rapidly decreases down to values similar to those of lower temperature pretreatments (case A). In both cases the carbon balance (calculated as  $\Sigma C$  atoms in products/ $\Sigma C$  atoms in converted butane) is lower than 100%. In case A it is sufficiently constant in the 80–90% range, whereas for the catalyst treated at a higher temperature (B) it is very low, especially in the first pulses (around 10%). An analogous marked carbon imbalance was observed by Pepera et al.<sup>4</sup> in a study of *n*-butane oxidation in a pulse reactor on vanadyl pyrophosphate. These authors utilized a higher concentration of *n*-butane in the pulses (about 46%). The analogy with literature data thus indicates the common aspect of the formation of carbon-containing species strongly held on the catalyst surface during pulse experiments.

**Fourier-Transform Infrared Spectra (FT-IR).** (a) **Interaction with C<sub>4</sub> Hydrocarbons.** *n*-Butane is adsorbed very weakly at room temperature (RT) on the surface of (VO)<sub>2</sub>P<sub>2</sub>O<sub>7</sub> (Figure 3, left) without strong vibration perturbation. However, if contact is carried out at higher temperatures (520–620 K), a relatively intense absorption may be observed in the region 1800–1500 cm<sup>-1</sup>. A main band is observed at 1620 cm<sup>-1</sup>, with a shoulder near 1710–1720 cm<sup>-1</sup> and another maximum at about 1780 cm<sup>-1</sup> (Figure 4a). No observable bands in the  $\nu_{CH}$  region correspond to these bands. The cited bands, reasonably related to  $\nu_{C=O}$  or  $\nu_{C=C}$  (possibly cyclic) species arising from the reactive adsorption of butane, are almost stable upon evacuation at temperatures up to 620 K. The relative intensity of the two higher frequency absorption bands depends strongly on the oxidation state of the catalyst, i.e., on the preliminary exposure time to oxygen and in vacuo. Figure 4b shows the spectrum obtained for a highly oxidized catalyst (only brief evacuation after the oxygen interaction).

Also but-1-ene is adsorbed weakly on the surface of vanadyl pyrophosphate at RT in a molecular form (Figure 3, right). The spectrum shows a weakening of the olefinic  $\nu_{CH}$ 's (3070 cm<sup>-1</sup>) and a shift of the  $\delta_{C=C}$  (from 1644 and 1648 for the *s-cis* and *gauche* conformers in the gas phase<sup>18</sup> to 1630 cm<sup>-1</sup>). These effects are

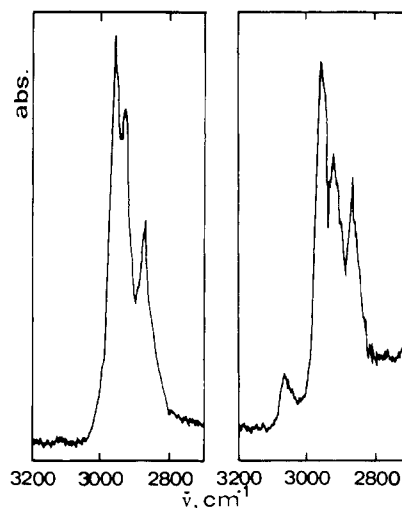


**Figure 3.** FT-IR spectra ( $\nu_{CH}$  region) of *n*-butane (left) and but-1-ene (right) adsorbed on (VO)<sub>2</sub>P<sub>2</sub>O<sub>7</sub> at room temperature.

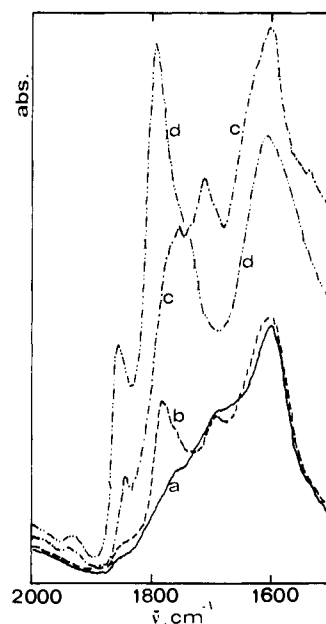


**Figure 4.** FT-IR spectra of the adsorbed species arising from *n*-butane adsorption in anaerobic conditions at 600 K on a (VO)<sub>2</sub>P<sub>2</sub>O<sub>7</sub> sample treated in oxygen at 620 K (1 h) and evacuated for 4 h at 620 K (a) or evacuated for 0.5 h at 620 K (b), and FT-IR spectra of the adsorbed species arising from but-1-ene adsorption in anaerobic conditions at 600 K on the vanadyl pyrophosphate evacuated for the longer time (c) and successively heated in oxygen (200 Torr) at 570 K for 1 h (d).

typical of the interaction of olefins, including but-1-ene, on Lewis acid sites.<sup>18</sup> A rather broad band in the region 1650–1600 cm<sup>-1</sup> is already apparent at RT. If contact is carried out at higher temperatures (520–620 K), a strong band is present at 1620 cm<sup>-1</sup>, with a shoulder at 1780 cm<sup>-1</sup> and another maximum at 1715 cm<sup>-1</sup> (Figure 4c), for interaction with a catalyst evacuated for long time. After further contact with oxygen (Figure 4d), the spectrum becomes very similar to that detected after contact with *n*-butane on a sample evacuated for short time (Figure 4b).

The interaction of the activated catalyst surface with buta-1,3-diene gas causes, already at RT, the formation of a spectrum very similar to that described above as a result of the high-temperature reactive adsorption of *n*-butane and but-1-ene. No features arising from molecularly adsorbed C<sub>4</sub>H<sub>6</sub> were observed under these conditions.

(19) Centi, G.; Fornasari, G.; Trifirò, F. *J. Catal.* **1984**, *89*, 44.

(20) Centi, G.; Trifirò, F. Preprints of Symposium on Hydrocarbon Oxidation, 194th National Meeting of the American Chemical Society, New Orleans, 1987 (Division of Petroleum Chemistry); p 754.

(18) Busca, G.; Ramis, G.; Lorenzelli, V.; Janin, A.; Lavalley, J. C. *Spectrochim. Acta, Part A* **1987**, *43*, 489.

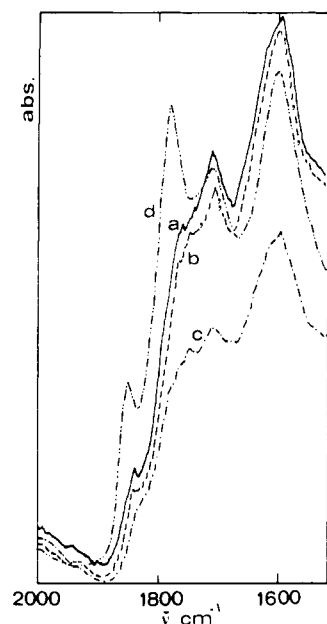


Figure 5. FT-IR spectra of the adsorbed species arising from but-1-ene adsorption at 600 K on  $(VO)_2P_2O_7$  (evacuated sample in contact with 20 Torr of but-1-ene gas) in the absence of oxygen and successively heated under evacuation at 520 K (a), 590 K (b), and 670 K (c). The other spectrum (d) is of but-1-ene adsorbed on a sample previously treated in oxygen at 620 K for 2 h and only briefly evacuated (0.5 h at 620 K).

In summary, the interaction of the three  $C_4$  hydrocarbons at 520–620 K produces the same spectrum. In all cases it is sensitive to the oxidation state of the catalyst, due to species arising from reactive adsorption. The reactivity scale is buta-1,3-diene > but-1-ene > *n*-butane, in agreement with that measured in a flow reactor under conditions of maleic anhydride synthesis.<sup>19–21</sup>

**(b) Behavior of the Adsorbed Species in Oxygen and in Vacuo.** If the samples evacuated for the longer time and successively put into contact in anaerobic conditions with the  $C_4$  hydrocarbons (620 K) are later put into contact with oxygen (200 Torr) at the same temperature, the spectrum is progressively modified. The band at  $1715\text{ cm}^{-1}$  initially decreases in intensity, while the sharp band at  $1780\text{ cm}^{-1}$  and its shoulder at  $1850\text{ cm}^{-1}$  increase considerably in intensity (Figure 4d). Later, also the stronger band begins to decrease slowly, while the two bands at 1850 and  $1780\text{ cm}^{-1}$  are still growing. These last bands are typical of  $\nu_{C=O}$  modes of cyclic anhydrides.<sup>22</sup> It seems then reasonable to deduce that large amounts of maleic anhydride are formed under these conditions. However, it should be noted that the intensity of these bands may be very strong even in the absence of gas-phase oxygen, if interaction is carried out on a sample that has previously been activated in oxygen at 620 K and evacuated briefly (Figures 4b and 5d). It seems then that maleic anhydride also forms on an oxidized surface (interaction with oxygen and brief evacuation) and not only in the presence of the gas-phase  $O_2$ . It must be noted that gas-phase  $CO_2$  is also detected if the oxidation is carried out in the presence of  $O_2$ .

From their behavior with oxygen it can be deduced that the bands at  $1715$  and  $1620\text{ cm}^{-1}$  are due to two different species, probably both acting as intermediates in the formation of maleic anhydride via different mechanisms.

The evacuation at temperatures up to 620 K of samples after contact with butane, butene, or butadiene at temperatures near 520–620 K only slowly affects the bands of adsorbed species. At temperatures near 670 K all bands begin to decrease slowly (Figure 5a–c).

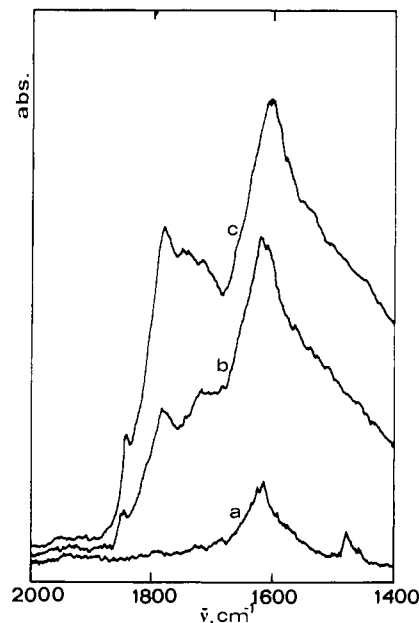


Figure 6. FT-IR spectra of the adsorbed species arising from 2,5-dihydrofuran adsorption on  $(VO)_2P_2O_7$  at room temperature (a), 480 K (b), and 590 K (c).

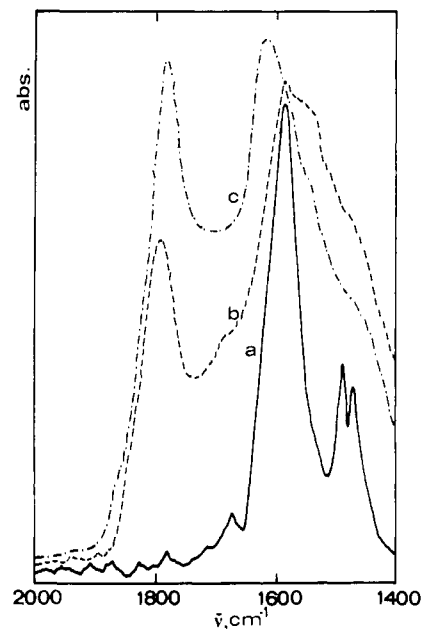


Figure 7. FT-IR spectra of the adsorbed species arising from furan adsorption on  $(VO)_2P_2O_7$  at room temperature (a), 480 K (b), and 590 K (c).

**(c) Interaction of Furan and 2,5-Dihydrofuran (DHF).** The spectra of the adsorbed species arising from the reactive adsorption of 2,5-dihydrofuran and of furan under similar conditions are compared in Figures 6 and 7. Weak bands are observed after DHF adsorption at RT. However, the spectra obtained by adsorption at higher temperatures are very similar to those obtained by adsorption of  $C_4$  linear hydrocarbons. In particular it can be noted that, together with the bands at  $1620\text{ cm}^{-1}$  and those of maleic anhydride ( $1840\text{ cm}^{-1}$  weak shoulder, and  $1780\text{ cm}^{-1}$ ), the band at  $1715\text{ cm}^{-1}$  is also present (Figure 6). Furan adsorbed at RT is characterized by bands similar to those measured for furan in a  $CCl_4$  solution,<sup>23</sup> although a strong intensity inversion is observed between the bands at  $1590$  and  $1485\text{ cm}^{-1}$ . These bands are very weak in the spectrum of furan adsorbed on alkali

(21) Centi, G.; Trifirò, F. *J. Mol. Catal.* **1986**, *35*, 255.

(22) Bellamy, L. J.; Connelly, B. R.; Philpotts, A. R.; Williams, R. L. *Z. Electrochem.* **1960**, *64*, 563.

(23) Loisel, J.; Pinan-Lucarre, J.-P.; Lorenzelli, V. *J. Mol. Struct.* **1973**, *17*, 341.

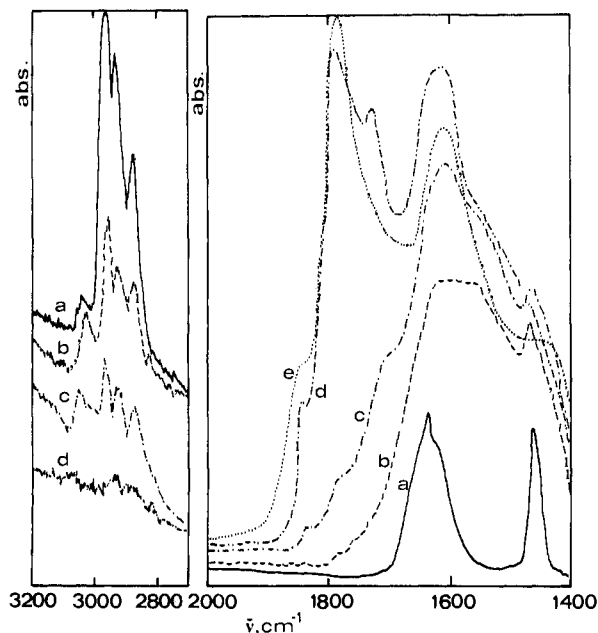


Figure 8. FT-IR spectra of the adsorbed species arising from the adsorption of pent-1-ene on  $(VO)_2P_2O_7$  at room temperature (a), 430 K (b), 590 K (c) and after treatment in oxygen (200 Torr) at 590 K (d) and 620 K (e).

halogenides.<sup>24</sup> The strong vibration perturbation indicates that the interaction involves not only the basic oxygen atom, but also the aromatic electron cloud. A considerable modification occurs in the spectrum at 480 K. A broad intense band is observed centered near  $1570\text{ cm}^{-1}$ , and a strong band is also present at  $1790\text{ cm}^{-1}$ . At 590 K the spectrum becomes similar to the usual one obtained from the other  $C_4$  compounds, the most intense band being shifted to  $1620\text{ cm}^{-1}$ .

However, the bands of maleic anhydride are very intense while the band at  $1715\text{ cm}^{-1}$  is absent. We may then conclude that furan adsorbed strongly as such at RT undergoes at higher temperatures some transformation producing the species characterized by the broad band at  $1570\text{ cm}^{-1}$ , and may later produce the same adsorbed species arising from the reactive adsorption of DHF and  $C_4$  hydrocarbons also with formation of maleic anhydride.

**(d) Interaction of  $C_5$  Hydrocarbons.** The interaction of  $C_5$  linear olefin with the vanadyl pyrophosphate gives spectra strictly correlated to those of  $C_4$  compounds (Figure 8). At RT a molecularly adsorbed species is observed, characterized again (as in the case of but-1-ene) by the weakening of the olefinic  $\nu_{CH_2}$  and by the shift of the  $\delta_{C=C}$ . At 430 K a broad absorption apparently with two maxima at  $1620$  and  $1560\text{ cm}^{-1}$  occurs, but the methyl group is still present ( $\nu_{CH_3}$  bands at the  $3000\text{--}2800\text{ cm}^{-1}$  region and the  $\delta_{CH_3}$  mode at  $1465\text{ cm}^{-1}$ ). At 480 K shoulders occur at  $1780$  and  $1710\text{ cm}^{-1}$ , while the component at  $1620\text{ cm}^{-1}$  predominates over that at  $1560\text{ cm}^{-1}$ . At 590 K the bands due to cyclic anhydrides are quite evident, but the band at  $1715\text{ cm}^{-1}$  also is very strong and that at  $1560\text{ cm}^{-1}$  has almost completely disappeared. Only at this temperature have the bands due to aliphatic  $CH_3$  groups almost completely disappeared. In contact with oxygen the amount of anhydride increases considerably at the expense mainly of the species responsible for the band at  $1715\text{ cm}^{-1}$ . Even in this case pretreatment of the sample in oxygen favors the formation of maleic anhydride.

**Desorption Studies.** The "stopped-flow desorption" (SFD)<sup>16</sup> technique was used to analyze the nature and evolution of the adsorbed species. SFD tests were carried out for  $n$ -butane oxidation and the products of desorption were analyzed according to the procedure described in the Experimental Section. Reported in Figure 9 is a typical chromatogram obtained for the fraction of products desorbed in the  $623\text{--}723\text{ K}$  temperature range

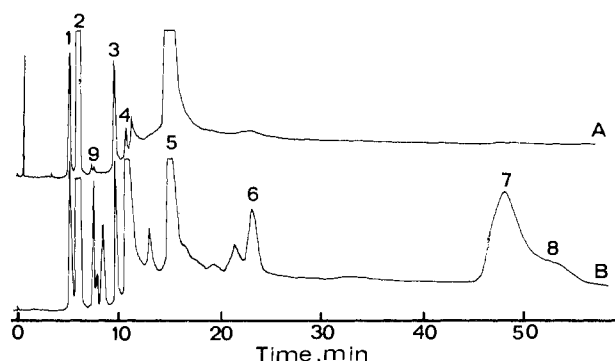


Figure 9.  $n$ -Butane oxidation at the vanadyl pyrophosphate surface: comparison of a typical chromatogram of the products of continuous-flow (2% butane in air) reaction (only organic products) (A) with the products (B) of thermal desorption in an unreactive flow in SFD experiments after the A stage. Legend: (1) acetaldehyde, (2)  $C_4$  hydrocarbons, (3) acetic acid, (4) crotonaldehyde, (5) maleic anhydride, (6) benzaldehyde, (7) phthalic anhydride, (8) phthalic acid, (9) furan.

Table III. Main Products (Except Carbon Oxides) Found during Desorption in a Deoxygenated Helium Stream after Steady-State Catalytic Tests in  $n$ -Butane Oxidation (Reaction Temperature, 573 K) on Vanadyl Pyrophosphate

desorption conditions	products of partial oxidation, $\text{mol} \times 10^7\text{ g}^{-1}$ of catalyst <sup>a</sup>				
	C4	AC	MA	CR	PA
(a) isothermal, 2 h <sup>b</sup> at 573 K	1.6	0.5	5.1		
(b) heating up to 723 K after step a		0.4	0.5	4.3	1.7

<sup>a</sup> C4,  $C_4$  hydrocarbons, mainly butadiene; AC, acetic acid and acetaldehyde; MA, maleic anhydride; CR, crotonaldehyde; PA, phthalic anhydride and acid. <sup>b</sup> After an initial 5 min of treatment in helium, in order to purge the line and to remove weakly adsorbed species.

Table IV. Main Products of Partial Oxidation after Desorption in Helium Flow after Oxidation of  $n$ -Butane in the Absence of Gaseous Oxygen at 573 K (Pulse Reactor)<sup>a</sup>

pulses	products of partial oxidation, $\text{mol} \times 10^8\text{ g}^{-1}$ of catalyst <sup>b</sup>				
	C4	MA	CR	PA	global amount
only butane <sup>c</sup>	1.2	0.6	6.3	1.2	9.5
butane + air <sup>d</sup>		1.2	0.5	1.4	3.2

<sup>a</sup> Range of desorption temperatures,  $573\text{--}723\text{ K}$ . <sup>b</sup> See footnote a in Table III for abbreviations. <sup>c</sup> Desorption after 8 pulses of  $n$ -butane/helium. <sup>d</sup> Desorption after 8 pulses of  $n$ -butane/helium and 2 consecutive pulses of air.

(chromatogram B); for comparison, a typical chromatogram (A) of the reaction products obtained in the continuous flow oxidation of  $n$ -butane (steady-state) at 573 K is also reported. Compared to continuous flow oxidation, a greater number of products of partial oxidation can be identified under SFD conditions, especially in the fraction desorbed at higher temperatures (the reaction temperature is 573 K). Reported in Table III are the moles per gram of catalyst for the principal products of mild oxidation formed. In particular, the additional presence of crotonaldehyde and of phthalic acid and anhydride in the fraction desorbed at higher temperatures as compared to that for steady-state oxidation is shown. In the lower temperature desorbed fraction, the principal products are  $C_4$  hydrocarbons (mainly butadiene). No olefins or diolefins were, on the contrary, detected in the outlet stream during  $n$ -butane oxidation in the flow reactor.

Similar results were obtained (Table IV) when the products of desorption were analyzed after anaerobic catalytic tests (pulse reactor). In this case, the principal product of mild oxidation is crotonaldehyde. When some pulses of air at 573 K are sent before the desorption, a decrease in the global amount of desorbed products is observed. The decrease is mainly due to the formation of  $CO_x$ . However, the formation of maleic anhydride in the products formed after the pulses of air is also revealed. This

**Table V.** Main Products of Partial Oxidation Determined after Desorption in Helium Flow after Steady-State Oxidation at 573 K of Butadiene and Furan

reagent	desorption conditions <sup>b</sup>	products of partial oxidation, mol × 10 <sup>7</sup> g <sup>-1</sup> of catalyst <sup>a</sup>				
		C4	FU	CR	MA	PA
butadiene	a	25.2	2.1	0.1	9.8	0.1
butadiene	b	0.6	0.1	27.7	1.5	8.1
furan	c	0.1	26.6	9.8	9.9	0.1

<sup>a</sup> See footnote a on Table III for abbreviations: FU, furan.

<sup>b</sup> Desorption conditions: (a) isothermal, 2 h at 573 K; (b) heating up to 723 K after step a; (c) steps a + b.

indicates that adsorbed species present on the catalyst surface may react with gaseous oxygen giving principally carbon oxides, but also partially transforming to anhydrides.

The SFD analysis of the products of desorption after the continuous-flow oxidation of butadiene (Table V) shows similar results. As compared to *n*-butane, a higher global amount of products of mild oxidation is found in the case of butadiene, indicating a much stronger interaction with the catalyst surface of the dienic hydrocarbon as compared to the paraffinic hydrocarbon. Anaerobic pulse reactor tests at 573 K confirm the strong interaction of butadiene. Unreacted butadiene, products of mild oxidation (mainly crotonaldehyde and maleic anhydride), and these of total oxidation (carbon oxides) were detected only after at least 15 pulses of butadiene (each pulse  $9.12 \times 10^{-7}$  mol of butadiene in helium) were sent onto the catalyst. This indicates that all corresponding hydrocarbon (or its products of oxidation) remains strongly held on the catalyst surface at 573 K. Successive desorption up to 723 K reveals a spectrum of products analogous to that found in similar tests in *n*-butane oxidation in the pulse reactor. Also in this case the main product of desorption in crotonaldehyde.

The SFD analysis after continuous-flow oxidation of furan to maleic anhydride (Table V) shows, together with large amounts of furan (C<sub>4</sub>H<sub>4</sub>O) and smaller amounts of the oxidation product, maleic anhydride (C<sub>4</sub>H<sub>2</sub>O<sub>3</sub>), the presence of reduced species as crotonaldehyde (C<sub>4</sub>H<sub>6</sub>O) in large amounts, and butadiene (C<sub>4</sub>H<sub>6</sub>) in smaller amounts. These data suggest that a disproportion reaction between adsorbed species occurs. The hydrogen atoms extracted from the intermediate during the mechanism of oxidation hydrogenate other adsorbed species, allowing the formation of crotonaldehyde and of butadiene from furan (H transfer mechanism through strongly adsorbed species). Only traces of phthalic anhydride are detected in the product of desorption after furan oxidation.

## Discussion

The data in Table I show that the presence of an additional carbon atom in the alkane chain causes a drastic change in the surface reactivity of vanadyl pyrophosphate. The synthesis of phthalic anhydride involves the formation of C–C bonds together with reaction of oxygen insertion. Gas-phase reactions are not involved in this synthesis.<sup>9</sup> Therefore, the surface dynamics of adsorbed species seem to play a specific role in the selective oxidation mechanism.

The nature of adsorbed species formed by the interaction of C<sub>4</sub> hydrocarbons with (VO)<sub>2</sub>P<sub>2</sub>O<sub>7</sub> has already been studied using infrared spectroscopy.<sup>25–28</sup> Rozhkova et al.<sup>27</sup> identified a band near 1600 cm<sup>-1</sup> as a surface carbonate. Puttock and Rochester<sup>26b</sup> attributed the same band to surface carboxylate. Wenig and

Schrader<sup>25</sup> attributed the band at 1600–1650 cm<sup>-1</sup> to  $\nu_{C-C}$  in C<sub>4</sub> olefins and a band at 1715 cm<sup>-1</sup> to  $\nu_{C=O}$  in maleic acid. Both molecules were suggested to be reactive intermediates, even though their surface concentration increased as a function of time on stream during in situ FT-IR studies.<sup>25</sup> Maleic acid has been suggested to be intermediate in the oxidative degradation of maleic anhydride.<sup>29</sup> Ramstetter and Baerns,<sup>28</sup> also using in situ FTIR spectroscopy, suggested the formation of 2,5-furanone.

The strong discordances between the interpretations of the same bands as well as the observation of their increase in intensity as a function of time on stream show that the surface characteristics of vanadyl pyrophosphate during catalytic reaction are much more complex than suggested in the literature. Furthermore, the simple IR observation of adsorbates does not allow the direct attribution of their role in the dynamics of transformation. The present data provide more information regarding these aspects, in relation also to the problem of the formation of the C<sub>8</sub> anhydride from the C<sub>5</sub> alkane.

**Nature of Adsorbed Species.** Desorption studies indicate the presence of relevant amounts of strongly adsorbed species on the surface of vanadyl pyrophosphate. These species form during the continuous-flow reactor (CFR) oxidation and thus in the presence of gaseous oxygen (Table III). Similar conclusions may be drawn from the lack of carbon balance in the pulse reactor experiments as well from the consecutive desorption tests. The higher temperature of desorption with respect to reaction temperature (573 K) suggests that the adsorbed species are strongly held on the surface and their turnover number is lower than that of the reaction intermediates. This means that their lifetime on the surface is long. It is worth noting that under these conditions relevant amounts of phthalic anhydride are detected in the desorption products of *n*-butane and butadiene CFR oxidation, whereas only traces are found in the desorption products of furan CFR oxidation.

All these indications may be summarized as follows. (a) The formation of phthalic anhydride also is possible from *n*-butane and butadiene, but requires a longer lifetime for the surface species to allow their interaction rather than direct oxidation to form maleic anhydride. On the contrary, only traces of phthalic anhydride can be detected in the desorption products of furan CFR oxidation.

(b) Probably two reaction pathways with different dynamics operate in the transformation of the C<sub>4</sub> hydrocarbons. The presence of adsorbed substances which desorb only at temperatures higher than the reaction temperature suggests that their reactivity is reduced as compared to intermediates directly involved in the synthesis of maleic anhydride. On the other hand, Table IV shows that the interaction of oxygen with these adsorbed substances leads to the formation of maleic anhydride together with carbon oxides (in a larger amount). Desorption studies thus suggest the presence of two oxidation pathways characterized by different dynamics, both leading to maleic anhydride synthesis. The slower one, involving the more strongly interacting adsorbed species, is also probably less selective owing to an enhanced probability for the formation of carbon oxides from adsorbed species with higher surface lifetimes.

The analysis of the FT-IR data and in particular of the behavior of adsorbed species in vacuo and in oxygen also shows a more complex surface situation than that reported in the literature.<sup>25–28</sup> When the surface is in an oxidized state or in the presence of gaseous O<sub>2</sub>, the typical bands for maleic anhydride are detectable. The reaction with the oxidized surface already is detectable at RT in the case of butadiene, while heat is necessary in the case of other hydrocarbons. The analysis of the infrared spectra indicates the presence of three adsorbed species in addition to maleic anhydride (species IV). They are characterized by bands at 1570 (broad, species I), 1620 (broad, species II), and 1715 cm<sup>-1</sup> (sharp, species III), possibly with a shoulder at 1780 cm<sup>-1</sup>, coinciding with the stronger band of maleic anhydride (species IV). Apparently,

(25) (a) Wenig, R. W.; Schrader, G. L. *J. Phys. Chem.* **1986**, *90*, 6480. (b) Wenig, R. W.; Schrader, G. L. *J. Phys. Chem.* **1987**, *91*, 1911. (c) Wenig, R. W.; Schrader, G. L. *J. Phys. Chem.* **1987**, *91*, 5674.

(26) (a) Puttock, S. J.; Rochester, C. H. *J. Chem. Soc., Faraday Trans. 1* **1986**, *82*, 2773. (b) Puttock, S. J.; Rochester, C. H. *J. Chem. Soc., Faraday Trans. 1* **1986**, *82*, 3013. (c) Puttock, S. J.; Rochester, C. H. *J. Chem. Soc., Faraday Trans. 1* **1986**, *82*, 3033.

(27) Rozhkova, E. V.; Gerei, S. V.; Gorokhovatskii, Ya. B. *Kinet. Catal. (Engl. Transl.)* **1975**, *15*, 618.

(28) (a) Ramstetter, A.; Baerns, M. *J. Catal.* **1988**, *109*, 303. (b) Do, M. T.; Baerns, M., personal communication.

(29) Moser, T. P.; Wenig, R. W.; Schrader, G. L. *Appl. Catal.* **1987**, *34*, 39.



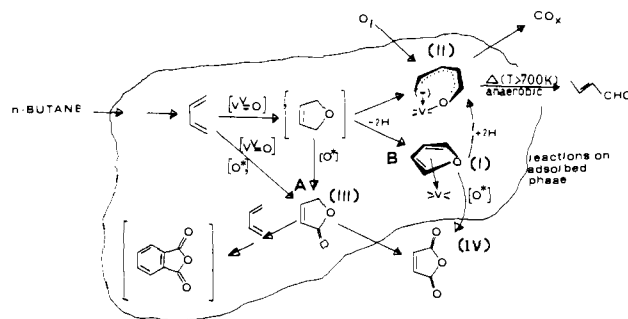
species I is rather unstable and evolves to species II with the parallel formation of maleic anhydride. It is formed in relevant amounts mainly from furan. Species III seems to convert more rapidly to maleic anhydride, and is not present after interaction of furan with the catalyst surface.

The similarity of the spectra obtained from butadiene and DHF suggests that the diene molecule may undergo a 1,4 addition by an oxygen species.<sup>21</sup> The interaction of buta-1,3-diene on iron and titanium oxides<sup>30</sup> forms an adsorbed *s*-trans molecular species, which upon heating produces carboxylate species, which later burn at high temperatures. On titania-supported vanadia<sup>31,32</sup> and molybdena<sup>33</sup> "monolayer" catalysts, on the contrary, maleic anhydride is formed from butadiene. In both cases the presence of vanadyl or molybdenyl surface groups completely changes the reactivity of the TiO<sub>2</sub> surface toward butadiene. Carboxylates are not observed. In both cases maleic anhydride is observed spectroscopically after reaction with gas-phase oxygen. It seems then reasonable that butadiene is oxidized by interaction with coordinatively unsaturated M=O (M = V, Mo) surface groups, able to cause 1,4 electrophilic addition of (formally) neutral oxygen atoms. This explains the analogy of the spectra from reactive adsorption of butadiene and unreactive (RT) adsorption of DHF. The products of DHF adsorption at higher temperatures (such as 480 K) have probably already undergone some transformations. From DHF, species II and III are very evident, together with maleic anhydride. The main band of species III is observed at 1715 cm<sup>-1</sup>, probably with a shoulder at 1780 cm<sup>-1</sup> and reasonably may be attributed to a stretching of a C=O bond. The presence of a split  $\nu_{C=O}$  band supports the identification of species III as an unsaturated lactone<sup>34</sup> (very probably the oxocyclopent-3-en-2-one) whose adsorption produces similar bands. This assignment is also supported by the lack of formation of species III from furan. In fact, the formation of such a lactone from furan would involve an improbable hydrogen migration from position 2 to 5, together with the insertion of one oxygen. The interpretation is in agreement with data of Baerns and Ramstetter,<sup>28</sup> whereas the assignment by Schrader et al.<sup>25,29</sup> to maleic acid is clearly not supported.

Species I and II, which appear to constitute the low- and high-temperature form of a similar species, are very probably strictly correlated with the furan molecule. Species I and II also form from DHF and C<sub>4</sub> hydrocarbons. Crotonaldehyde is a significant component in the desorption products of all such compounds including furan. Therefore, it is possible to propose that species I is a strongly adsorbed species of intact furan (according to the detection of very high amounts of furan such as in the desorption products of its steady-state oxidation), while species II might be a related hydrogenated open form that thermally evolves to crotonaldehyde. Hydrogenation of furan through hydrogen transfer may occur during the oxidation of a parallel adsorbed furan molecule to maleic anhydride. The formation of species II from furan in FT-IR spectra is, in fact, parallel to the detection of the bands of the maleic anhydride. The observed band (1620 cm<sup>-1</sup>) may justify the assignment to some kind of enolic form, according to the similar spectra observed for the enolic form of acetone adsorbed on Fe<sub>2</sub>O<sub>3</sub><sup>35</sup> and of enol in metal complexes.<sup>36</sup>

**Selective Pathways of Oxidation.** Analysis of the FT-IR spectra suggests a first path to maleic anhydride involving the intermediate formation of adsorbed DHF and of the corresponding lactone,

**Scheme I.** Proposed Reaction Pattern in *n*-Butane Selective Conversion to Maleic Anhydride on Vanadyl Pyrophosphate



in good agreement with the results of Ramstetter and Baerns.<sup>28</sup> This first path to maleic anhydride is apparently the faster one, as indicated by the higher reactivity in the presence of gaseous oxygen. As discussed before, desorption data suggest that a second slower pathway of maleic anhydride synthesis also is present. The data in Table IV indicate that strongly adsorbed species may also produce maleic anhydride, even though this second mechanism probably is less selective. Accordingly, "temporal analysis of products" (TAP) experiments with labeled molecules indicate that in the oxidation of butane strongly adsorbed species may be precursors for the formation of carbon oxides due to their enhanced surface lifetime.<sup>37-39</sup> FT-IR data indicate a specific role of furan in the formation of these strongly adsorbed species and that furan can generate maleic anhydride, according to flow reactor<sup>21</sup> and spectroscopic studies.<sup>26</sup> However, as shown in Table V, furan does not form phthalic anhydride. This is further evidence that two oxidation pathways operate at the vanadyl pyrophosphate surface.

In summary, the reaction pattern reported in Scheme I can be proposed for the synthesis of maleic anhydride from C<sub>4</sub> hydrocarbons. Oxygen insertion with consecutive dehydrogenation (route B) or direct insertion of two oxygen atoms (route A) on the intermediate butadiene would probably involve a different surface distribution of oxygen insertion sites. If, in the oxygen insertion step, the lattice V<sup>V</sup>=O sites are assisted by an additional labile oxygen species [O\*] (called labile in order to evidence its enhanced reactivity, according to notation previously discussed<sup>5a,37-39</sup>), the lactone forms directly (route A). If only the V<sup>V</sup>=O sites near to the adsorbed butadiene are present, the oxidation proceeds through oxygen insertion and consecutive dehydrogenation (route B). It should be mentioned that we have already noted that dehydrogenation of 2,5-dihydrofuran to furan occurs at very low reaction temperatures on vanadyl pyrophosphate.<sup>21</sup> Furan may also be oxidized to maleic anhydride<sup>21</sup> but, because of its strong interaction with surface Lewis acid sites as evidenced by FT-IR spectra (Figure 8), may act also as a surface H-transfer agent with its partial conversion to a strongly interacting hydrogenated surface species (II), possible precursor of formation of carbon oxides.

This reaction scheme is also supported both by FT-IR and catalytic results on the oxidation of C<sub>5</sub> hydrocarbons. The FT-IR spectra show that the adsorbed species arising from C<sub>5</sub> hydrocarbons are strictly analogous to those arising from C<sub>4</sub> molecules. However, in that case the bands due to species III and maleic anhydride seem to be always stronger relative to those of species II and I. Moreover, also the relative intensity of the band due to species III seems enhanced with respect to maleic anhydride, generally, in the case of C<sub>5</sub> molecules. This would be due to the fact that the presence of the side methyl group in the methyl DHF results in a further inhibition of the formation of species I and

(30) (a) Busca, G.; Marchetti, L.; Zerlia, T.; Girelli, A.; Sorlino, M.; Lorenzelli, V. In *Proceedings of the 8th International Congress on Catalysis, Berlin, 1984*; Dechema: Frankfurt am Main, 1984; Vol. III, p 299. (b) Busca, G.; Porcile, G.; Lorenzelli, V. *J. Mol. Struct.* **1986**, *141*, 395.

(31) Busca, G.; Centi, G.; Marchetti, L.; Trifirò, F. *J. Chem. Soc., Faraday Trans. 1* **1985**, *81*, 1003.

(32) Busca, G.; Centi, G.; Marchetti, L.; Trifirò, F. *Langmuir* **1986**, *2*, 568.

(33) Ramis, G.; Busca, G.; Lorenzelli, A. *Appl. Catal.* **1987**, *32*, 305.

(34) Jones, R. N.; Angell, C. L.; Ito, T.; Smith, R. J. D. *Can. J. Chem.* **1959**, *37*, 2007.

(35) Busca, G.; Lorenzelli, V. *J. Chem. Soc., Faraday Trans. 1* **1980**, *78*, 2911.

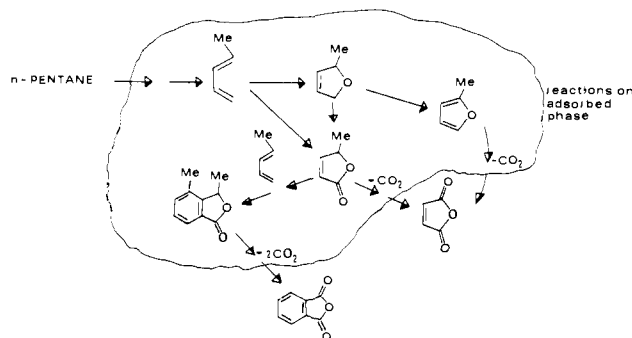
(36) Koga, O.; Onishi, T.; Tamaru, K. *J. Chem. Soc., Faraday Trans. 1* **1980**, *76*, 19.

(37) Centi, G.; Trifirò, F.; Busca, G.; Ebner, J. R.; Gleaves, J. T. In *Proceedings of the 9th International Congress on Catalysis, Calgary, Canada, 1988*; Vol. IV, p 1538.

(38) Gleaves, J. T.; Ebner, J. R.; Kuechler, T. C. *Catal. Rev.-Sci. Eng.*, in press.

(39) Ebner, J. R.; Gleaves, J. T. In *Proceedings of the 5th IUCCP Symposium on Oxygen Complexes and Oxygen Activation by Metal Complexes*, College Station, Texas, March 1987.



**Scheme II.** Proposed Reaction Pattern in *n*-Pentane Selective Conversion to Maleic and Phthalic Anhydrides on  $(VO)_2P_2O_7$ 

II (and eventually to maleic anhydride via furan oxidation). This is very reasonable because of the difficulty of oxidative decomposition of such a methyl group. This is also confirmed by the absence of  $C_5$  oxidation products, which would imply difficulty of the vanadyl pyrophosphate in the insertion of oxygen in allylic positions (such as on the hypothesized penta-1,3-diene to form, for example, 2,4-pentadienoic acid or the corresponding aldehyde). This is more evident from the absence of products of allylic oxygen insertion (acrolein, acrylic acid) from propane, as previously reported.<sup>20</sup> The proposed reaction pattern of anhydride formation reported in Scheme I, on the contrary, does not involve this type of oxygen insertion in the mechanism of synthesis. Moreover, the presence of the side methyl group in the lactone molecule (species III) favors its stability toward oxidation to maleic anhydride and eventually its detection by FT-IR, as well as its availability to undergo a surface template reaction with the diene molecule. We may remark that desorption studies clearly indicate the presence of relevant amounts of adsorbed diolefins during alkane oxidation. IR detection of  $\nu_{C=C}$ , however, is based on the presence of a broad band below  $1600\text{ cm}^{-1}$  which in this case is probably covered by other bands. This may explain the much higher productivity of phthalic anhydride from  $C_5$  than from  $C_4$  hydrocarbons during the continuous-flow reactor experiments. After the formation of C-C bonds, oxidation of the methyl groups is easier, since such groups are now bonded to benzylic positions. Lateral methyl groups in activated aromatics are easily oxidized on vanadyl pyrophosphate with consecutive decarboxylation. The proposed reaction pattern of *n*-pentane oxidation is reported in Scheme II. In agreement, because of the higher surface density of adsorbed species, an autocatalytic dependence on the oxygen partial pressure at the lower reaction temperatures (Figure 2) is found for the rates of formation of both anhydrides from *n*-pentane. Furthermore, as shown in Figure 2, the higher concentration of oxygen favoring the rate of direct oxidation, and thus decreasing the surface lifetime of adsorbed species (and their surface density), increases the probability of the formation of maleic anhydride from *n*-pentane in comparison to the reaction of synthesis of phthalic anhydride. The pulse reactor tests (Table II) confirm, in fact, the different role of oxygen in the oxidation of *n*-butane and *n*-pentane.

**Cocatalysis Effects.** Desorption studies evidence an important aspect of the surface chemistry of vanadyl pyrophosphate during catalytic reactions. The analysis of the products formed during furan oxidation (Table V) indicates that, together with oxidized products (maleic anhydride), hydrogenated products (crotonaldehyde and smaller amounts of butadiene) also are present on the surface. It is likely that the hydrogen atoms extracted from furan in the synthesis of maleic anhydride may also act as hydrogenation sites. This shows the role of the surface mobility of intermediates species in the reaction mechanism even in the presence of gaseous oxygen. Pepera et al.<sup>4</sup> in anaerobic experiments with labeled molecules also have proposed a surface model

based on the shuttling of hydrogen away from and oxygen toward the intermediate adsorbed and fixed on the surface until maleic anhydride is formed. It is also likely that the strongly adsorbed species may play the role of cocatalyst acting as hydrogen-transfer agents. We have already reported<sup>5a,16</sup> that during transient activation of vanadyl pyrophosphate the selectivity to maleic anhydride increases considerably with a parallel increase in the amount of strongly adsorbed species. We suggest that, parallel to their role as hydrogen-transfer agents, these strongly adsorbed species also may play a role in an oxygen-transfer mechanism. This hypothesis explains the previous observation and agrees with the observations of Pepera et al.<sup>4</sup>

We may therefore conclude that in addition to their role in the selective pathways of  $C_4$  and  $C_5$  alkane transformation, strongly adsorbed species significantly modify surface reactivity acting as cocatalysts and enhancing the surface mobility of simple species.

## Conclusions

The present data indicate that the nature of the vanadyl pyrophosphate surface during selective oxidation of  $C_4$  and  $C_5$  alkanes is more complex than previously reported in the literature.<sup>3a,5a</sup> In particular, the surface dynamics of adsorbed species play an important role in determining the nature of selective oxidation pathways and reaction products. Furthermore, cocatalysis effects induced by strongly adsorbed species also appear to have an effect on surface reactivity. This opens new perspectives in the understanding of the mechanisms of complex heterogeneous surface reactions and in the characterization of the real working state of catalyst surfaces.

In particular, for the *n*-butane conversion, two selective oxidation pathways to maleic anhydride are thought to be present involving the intermediate formation of either a lactone or furan by reaction of the adsorbed butadiene intermediate with  $V=O$  surface groups, possibly assisted in the synthesis of lactone by other labile oxygen species. The relative probabilities of these two pathways depend on the oxygen availability near this common intermediate. The two oxidation pathways are characterized by different rates of transformation to maleic anhydride and probably by different selectivities. The route through furan leads to the formation of strongly adsorbed species as possible precursors of carbon oxides. A small lowering of the reactivities of these intermediates, such as that deriving from the presence of an additional lateral methyl group, favors the possibility of a parallel side surface reaction between the intermediates of reaction which finally leads to phthalic anhydride from pentane when limited oxygen sites are available. At higher surface oxygen concentrations, maleic anhydride is the preferential product from pentane as in the case of butane.

In conclusion, surface reactivity measurements, Fourier-transform infrared studies, and stopped-flow desorption measurements suggest that the selectivity and the nature of the products of oxidation of  $C_4$  and  $C_5$  alkanes on  $(VO)_2P_2O_7$  is controlled by the dynamics of surface reactions at the vanadyl pyrophosphate surface. It is possible to induce new synthesis features by reducing the rate of some surface reactions, as shown by the synthesis of phthalic anhydride from *n*-pentane, a new type of heterogeneous oxidation reaction. This evidence further stresses the fundamental scientific interest in understanding surface dynamics and concentrations of adsorbed intermediates/species.

**Acknowledgment.** The Ministero Pubblica Istruzione (National Group on the Structure and Reactivity of Surfaces) is gratefully acknowledged for financial support.

**Registry No.** DHF, 1708-29-8;  $(VO)_2P_2O_7$ , 58834-75-6; *n*-butane, 106-97-8; maleic anhydride, 108-31-6; *n*-pentane, 109-66-0; phthalic anhydride, 85-44-9; but-1-ene, 106-98-9; buta-1,3-diene, 106-99-0; furan, 110-00-9.